# THE PUZZLING HARMONIC BEHAVIOR OF THE CATHEDRAL QPO IN XTE J1859+226

J. RODRIGUEZ[1] & P. VARNIÈRE[2]

*Draft version January 20, 2013*

## ABSTRACT

We present a spectral and temporal analysis of the Cathedral QPO detected in the power density spectra of the black hole binary and microquasar XTE J1859+226 obtained with *RXTE*. This peculiar type of QPO has been seen on two occasions (on MJDs 51574.43 and 51575.43) during the 1998 outburst of this source. It manifests as two peaks with similar amplitudes ($\sim 3\%$ and $\sim 5\%$ RMS) and harmonically related centroid frequencies ($\sim 3$ and $\sim 6$ Hz). The temporal properties of these two peaks are different: the amplitude of the $\sim 3$ Hz feature varies, in anticorrelation with the count rate, by about $\sim 50\%$. The $\sim 6$ Hz feature, on the other hand, shows a slight increase ($\sim 7\%$) of its amplitude with count rate. The RMS-spectra of the two peaks are also quite different. The $\sim 3$ Hz feature is softer than the other one, and although its RMS amplitude increases with energy it shows a cut-off at an energy of $\sim 6$ keV. The RMS of the 6 Hz increases up to at least 20 keV. We also study the bicoherence, $b^2(\mu, \nu)$ of both observations. At the diagonal position of the peaks the values $b^2(\sim 3, \sim 3)$ and $b^2(\sim 6, \sim 6)$ are rather high and similar to what has been reported in the case of the type C QPOs of GRS 1915+105. By comparison with the latter source the fact that the bicoherence of the $\sim 3$ Hz feature is higher than than of the other peak, would tend to indicate that the $\sim 3$ Hz is the fundamental QPO, and the other its first harmonic. The value of $b^2(\sim 3, \sim 6)$ is, however, low and therefore indicates a behavior that is different than that seen in GRS 1915+105. We discuss the implications of these differences in the context of an harmonic relationship of the peaks, and suggest that, rather than pure harmonics, we may see different modes of the same underlying phenomenon competing to produce QPOs at different frequencies.

*Subject headings:* accretion, accretion disks — black hole physics — stars: individual (XTE J1859+226, XTE J1550−564, GRS 1915+105) — X-rays: stars

## 1. INTRODUCTION

Black Hole Binaries (BHB, e.g. Remillard & McClintock 2006, for a review) transit through different 'spectral states' during their outbursts. These are defined both by the spectral and temporal parameters respectively obtained through analyses of their energy spectra and power density spectra (PDS). In the soft state, where the emission is dominated by a bright and warm ($\sim 1$ keV) accretion disk, the level of variability is weak, and the PDS is power law like. On the other hand, in the hard state, when the disk is much colder ($\leq 0.5$ keV) and thought to be truncated at a large distance from the accretor, the level of variability is much higher and shows a band limited noise component. Other states exist and can be seen as intermediate between the Hard and Soft ones. See e.g. Remillard & McClintock (2006); Homan & Belloni (2005) for recent reviews and precise classifications of the BHB's states. Furthermore, quasi-periodic oscillations in the 'low frequency' range (0.1–20 Hz, hereafter referred to as LFQPO) are seen in the hard and during the intermediate states. These LFQPOs have been further classified into types A, B, or C based on their typical frequencies, total RMS amplitude, and time lags (e.g. Remillard et al. 2002; Casella et al. 2005). We have recently proposed a tentative classification of states based on the presence of the different types of QPOs (Varnière et al. 2011).

The exact origin of QPOs is still a matter of debate: they could be due to global oscillations of the disk (e.g.

Wagoner et al. 2001, and ref. therein), Lense-Thirring precession (e.g. Ingram et al. 2009, and ref. therein), oscillating shocks (e.g. Molteni et al. 1996, and ref. therein), or MHD instability (Tagger & Pellat 1999). From the observational side it seems clear that the inner disk somehow sets the frequency of LFQPOs (e.g. Muno et al. 1999; Rodriguez et al. 2002a,b, 2004b; Mikles et al. 2009). LFQPOs are, however, strong when a strong hard component is seen in the energy spectra and their frequency is correlated with the power law photon index (e.g. Vignarca et al. 2003; Shaposhnikov & Titarchuk 2007). This last point would tend to indicate an origin in relation to the corona. The amplitude of QPOs increases with the energy up to a cut-off whose energy is variable (Rodriguez et al. 2004a, 2008).

These LFQPOs usually manifest in the PDSs as powerful peak referred to as the fundamental and a series of (sub) harmonics usually of much fainter amplitudes. Very little focus has been put so far on these harmonics, even if it is clear that they do not completely share the same properties as the fundamental. They can show different signs for their time lags, as in the case of type B QPOs (Casella et al. 2004), and show different shapes of the RMS spectra (Cui 1999; Homan et al. 2001; Rao et al. 2010). The true identification of the fundamental has recently been questioned (e.g. Rao et al. 2010), which raises questions related to the genuineness of the harmonic relationship of the peaks.

[1]Laboratoire AIM, UMR 7158, CEA/DSM - CNRS - Université Paris Diderot, IRFU/SAp, F-91191 Gif-sur-Yvette, France

[2]Laboratoire APC, UMR 7164, CNRS-Université Paris Diderot-CEA/DSM, 10 rue Alice Domon et Leonie Duquet, 75205 Paris Cedex 13, France.

XTE J1859+226 was discovered on 1999 October 9 with the *RXTE* All Sky Monitor (Wood et al. 1999) as it was entering into outburst. It is a microquasar given the observations of relativistic ejections in radio (Brocksopp et al. 2002), and the observations of low and high frequency QPOs led Cui et al. (2000) to classify it as a candidate BHB. An extensive timing analysis of this source is presented by Casella et al. (2004). Like XTE J1550−564, XTE J1859+226 displays all three types of LFQPOs. In two particular observations, during the 1999 outburst, Casella et al. (2004) observe the presence of two peaks with harmonically related frequencies, but unlike any other cases, similar RMS-amplitudes. These are referred to as the 'Cathedral' QPO (Casella et al. 2004): the strongest peak (and highest in frequency) has hard lags (the hard X-ray lag behind the soft X-rays) and is interpreted as the fundamental peak, while the lowest frequency peak has soft lags and is the sub-harmonic. Interestingly these two observations, although separated by about a day, are also separated by an observation showing another type of QPO indicative of a spectral transition (Casella et al. 2004).

The existence of this Cathedral QPOs showing two harmonically related peaks of similar amplitude raises challenging questions for all theoretical models. To obtain a clearer view of the properties of these peaks we performed a complete study of the QPO structure from these two observations, and compare the temporal and spectral behaviors of the two peaks. The organization of the letter is as follows: we start presenting the observations ID and data reduction methods. We then describe our results in Section 3, starting with the temporal evolution of the source, the fit to the broad band PDS, the energy dependences of the QPOs, and we end this part by presenting the bicoherence of the observations. We discuss our findings in the last section of this letter.

## 2. OBSERVATIONS AND DATA REDUCTION

We focus on *RXTE* observations 40124-01-24-00 (Obs. 1) and 40124-01-27-00 (Obs. 2) respectively made on 1999 october, 23 (MJD 51474.43) and 24 (MJD 51475.43), near the peak of the 1999 outburst. The full process of *RXTE*/PCA data reduction was made with the `HEASOFT v6.9` software package. We reduced the Binned and Event mode data following standard procedures (see e.g. Rodriguez et al. 2008) to obtain light curves filtered from low elevation above the Earth, large offset from the source, and PCU breakdown. We extracted $7.8125 \times 10^{-3}$ s binned light curves in several energy ranges used for the fine timing analysis , and a $\sim$ 2–15 keV light curve from the Binned data with a time bin of 8 s (Fig. 1) to characterize the overall behavior of the source over the observations. Note that this range contains most of the counts emitted by the source. Power density spectra (PDS) were then produced with `Powspec v1.0` on intervals of 16 s in the range 0.0625–64 Hz, all intervals being further averaged together before the fitting process. A dynamical PDS (DPDS) was also computed between 0.25 and 64 Hz, to study the variations of the QPOs with time (Fig. 1). The PDSs were fitted between 0.0625 and 40 Hz in `XSPEC v12.6.0`. The background rate was taken into account when estimating the RMS amplitudes of the different features following $A_{net} = A_{raw} \times \frac{S+B}{S}$, with $A$ the am-

plitude, $S$ is the source net rate, and $B$ the background rate (Berger & van der Klis 1994; Rodriguez et al. 2004a, 2008).

## 3. RESULTS

### 3.1. *Time evolution of the source: light curve and dynamical PDS*

The 2–15 keV XTE J1859+226 PCA light curve binned at 8 s and DPDS of Obs. 1 are reported in Fig. 1. Large variations around a mean raw (net) count rate of 5700 cts/s (5676 cts/s) are clearly visible. We especially note the presence of two rather broad dips lasting respectively $\sim$ 100 s and $\sim$ 50 s near relative times 1350 s and 1775 s, and a third occurring near the end of the observation (at t$\sim$ 2050 s). The DPDS shows the presence of two strong features (relatively to the overall noise) around 3 and 6 Hz. These two features are quite thin and indicate the presence of QPOs at these frequencies. Interestingly the two QPOs seem to have different behavior with time (Fig. 1): the QPO with the smallest frequency is, on average, much weaker than the other one, and is strong only when the count rate is around its mean value. It is, in particular quite weak during the small flares, and is not visible during the three dips. The highest frequency QPO, on the other hand, seems, in term of power, more stable and seems to vary significantly only during the dips (Fig. 1). The feature seems rather broad around $\sim$ 6 Hz, which may indicate some rapid variations of the frequency, or simply an intrinsically low coherence QPO. A very similar behavior (not shown) is also seen in both the light curve and DPDS of Obs. 2.

### 3.2. *Broad band PDS*

We started with fitting the large band PDSs. We did not subtract the white noise and preferred adding a constant to our fit model to account for this component. Following Casella et al. (2004) we fitted the continuum with the sum of three broad and three narrow Lorentzians (Fig. 2) on top of the white noise component. This model yields a good fit with $\chi^2_\nu$=1.13 (resp. 1.09) for 118 degrees of freedom (DOF) for Obs. 1 (resp. Obs. 2). The parameters of the three thin peaks are reported in Table 1 for both observations. The parameters of all three peaks are compatible between the two observations, which lends credence to their complete similarity. In the remainder of the paper only the results of Obs. 1 are precisely described and presented in the figures. Note that in all cases the same analysis was performed on Obs. 2 and the results and trends observed are consistent with those of Obs. 1. The third peak is compatible with $4 \times \nu_1$, and $2 \times \nu_2$ at the $\sim 2\sigma$ level, and is likely to be an harmonic of one of the two main peaks. In the remainder of this paper, we will refer to either peak 1, 2, or 3, or QPO 1, 2, or 3 for the peaks at $\sim$ 2.9, $\sim$ 5.8, and $\sim$ 11.2 Hz respectively.

Although the fit statistic is quite good, we remark some residuals on the lower shoulder of QPO$_2$. This effect is also mentioned by Casella et al. (2004) in Obs. 2, and these authors added a Gaussian to better represent the peak. In our case, the addition of another thin Lorentzian at $\sim$ 5.5 Hz improves the fit to $\chi^2_\nu$=0.90 for 137 DOF, and

corrects the defect previously present in the residuals. The feature is, however, poorly defined, and its parameters are badly constrained. We verify, by re-doing the whole analysis that it had no significant impact on the other peaks, and since no influence was found it was omitted from our study, and is not further discussed here.

As mentioned in the previous section, QPO$_1$ seems more intermittent that the second peak (Fig. 1). In order to quantify and study any possible dependence of the QPOs amplitudes with the count rate (Sec. 3.1), we followed a procedure similar to that presented in Heil et al. (2011). Each observation was separated into ten count rate intervals of equal width. Each interval therefore has a width equal to $\frac{Max(CR)-Min(CR)}{10}$ cts/s. Due to short accumulation times, and thus poor statistical quality of the resulting PDSs, some of pairs of intervals were combined together. In the case of Obs. 1 this rebin concerned intervals 1&2, and intervals 3&4. The final division of Obs. 1 is represented in Fig. 1. We then extracted a $7.8125 \times 10^{-3}$ s binned light curve per time interval of 8 s, and produced a PDS from each of these light curves. Individual PDSs belonging to the same count rate interval were averaged together to produce the final count rate dependent PDSs. The latter were then fitted to estimate the parameters of the peaks, with a special focus on their rms amplitudes. No specific trend is seen between the frequency or the coherence of any of the two peaks with the count rate. In order to ease the comparison with the QPOs of XTE J1550−564 (Heil et al. 2011), we represented the evolution of the absolute RMSs (in terms of cts/s) of the two peaks with the count rate in Fig. 3 for the particular case of Obs. 1. The amplitude of QPO$_1$ decreases with increasing count rate, while that of QPO$_2$ increases slightly (Fig. 3) and show a possible linear trend. Between the first real detections of the two peaks (in the second count rate bin) and the last bin, QPO$_1$ varies from an RMS amplitude of $2.7 \pm 0.3\%$ to $1.35 \pm 0.34$ (a variation of 50% in amplitude) while QPO$_2$ varies from $3.6 \pm 0.4\%$ to $3.9 \pm 0.2\%$ (a non-significant variation of $\sim 7.7\%$ in amplitude).

## 3.3. *Energy dependence of the QPOs*

To study the energetic dependence of the QPOs and produce the RMS-Spectra (Fig. 4), we fitted each energy dependent PDS with the statistically required number of broad features to account for the continuum. We remark here that these features also have complex energetic dependences, and thus the different fits either require 1,2, or 3 broad Lorentzians. The study of these is, however, beyond the scope of this letter and we will not discuss them further. We then added the thin Lorentzians to account for the QPO. The third peak is most of time undetectable and no spectrum can be acquired for it. The resultant RMS-Spectra for QPO$_1$ and QPO$_2$ from Obs. 1 are reported in Fig. 4. An almost identical behavior is seen in the QPO spectra obtained from Obs. 2 (not shown).

The two QPOs share a common trend: their amplitude first increases with energy before reaching a plateau. Such QPO-spectra are common for all types (A, B, C) of LFQPOs in this source (Casella et al. 2004), and have, for example, also been seen in GRS 1915+105 (Rodriguez et al. 2004a, 2008), and XTE J1550−564 (Homan et al. 2001; Rodriguez et al. 2004b). The fact that the normalization

of the spectra is different is not unexpected since the two peaks have different total amplitudes. The precise shape and typical parameters (energy of the break, slope, ...) are, however, clearly different (Fig. 4). This is illustrated in the right panel of Fig. 4, where we normalized the RMS spectrum of QPO$_2$ by that of QPO$_1$. This representation also clearly shows that QPO$_2$ has a steeper (harder) spectrum than QPO$_1$. The latter first increases up to $\sim 5.7$ keV and is then flat until $\sim 20$ keV. QPO$_2$ is undetectable in the first energy bin (and is thus fainter than QPO$_1$). It increases up to $\sim 20$ keV where its plateau is reached.

### 3.3.1. *Bicoherence of the Cathedral QPO*

The bispectrum and the related bicoherence permit any possible coupling between the different components of the PDS to be studied, and thus allow one to go beyond the diagnosis brought by the PDSs (see e.g. Maccarone et al. 2011, and references therein for a deeper discussion on these aspects). Dividing the light curve in K segments of equal length, the bicoherence is expressed as:

$$b^2(\nu,\mu) = \frac{|\sum_{i=0}^{K-1} X_i(\nu)X_i(\mu)X_i(\nu+\mu)|^2}{\sum_{i=0}^{K-1} |X_i(\nu)X_i(\mu)|^2 \times \sum_{i=0}^{K-1} |X_i(\mu+\nu)|^2}$$

where $X_i(\nu)$ is the $\nu$ component of the discrete Fourier transform of the $i^{th}$ interval (see e.g. Maccarone & Coppi 2002; Uttley et al. 2005; Maccarone et al. 2011, for the description, restriction, interpretation and applications to various astrophysical sources, including BHBs). We calculated the 2–15 keV bicoherences of XTE J1859+226 between $6.25 \times 10^{-2}$ Hz and 16 Hz, with a frequency resolution of 0.0625 Hz. Fig. 5 shows a zoom on the bicoherence plot we obtained in the case of Obs. 1 (the plots and results obtained in the case of Obs. 2 are almost identical). Note that by definition the bicoherence is symmetric with respect to the first diagonal ($b^2(\nu,\mu) = b^2(\mu,\nu)$). The highest values of the bicoherence are reached in a region around $(\nu_1,\nu_1)$ (the latter being indicated by the white box close to the bottom left corner in Fig. 5), between $\sim 2.8$ and $\sim 3.2$ Hz along the first diagonal (Fig. 5), with a slight broadening at low frequencies. A local maximum is also reached around the frequency of QPO$_2$ (illustrated by the second white box in Fig. 5). Note that the mean value of $b^2$ calculated in the white regions represented in Fig. 1 is higher around QPO$_1$ than around QPO$_2$. The mean value of $b^2$ over the 0.0625–16 Hz range is 0.008 with a an RMS of about 0.008. The value of $b^2$ around $(\nu_2,\nu_1)$ (black box in Fig. 5) is quite low. At the position of the two peaks we obtain $b^2(\nu_2,\nu_1) \sim 0.01$, a value within the statistical fluctuations around the mean of $b^2$, and clearly compatible with "noise". Note that the same results are obtained when looking at the mean value of $b^2$ in broad (e.g. $5 \times 5$ frequency-pixels) regions centered on $(\nu_2,\nu_1)$. Overall, this tends to show that either the two peaks are not coupled or that their coupling is very weak.

## 4. DISCUSSION AND CONCLUSIONS

We presented here an analysis of some of the properties of the peculiar 'Cathedral' QPO (Casella et al. 2004) seen in XTE J1859+226. Although we mainly focused here on Obs. 1 to illustrate our analysis, similar results and trends were obtained in the case of Obs. 2, allowing us to use these two observations in our argumentation. The

cathedral QPO manifests as two apparently harmonically-related peaks of similar amplitudes in the PDSs (Fig. 2). Casella et al. (2004) concluded that $QPO_2$ is the fundamental feature while $QPO_1$ is its 'sub'-harmonic. With this conclusion, and adding the fact that $QPO_2$ shows hard time lags while $QPO_1$ show soft time lags, they classify the Cathedrals as type B QPOs (Casella et al. 2004).

Although $QPO_1$ and $QPO_2$ seems to be harmonically related, and have been classified as harmonics, their overall behavior is quite different. We summarize here the main differences:

1. Their amplitude has a different temporal evolution. $QPO_2$ is present during the whole observation (apart from the 3 dips mentioned in Sec. 3.1), while $QPO_1$ is only intermittently seen. Our analysis shows that it undergoes larger variations of its amplitude than $QPO_2$ (Sec. 3.1).

2. The RMS-spectra of these two peaks are clearly different in shape, normalization and typical parameters (Fig. 4). In particular, the characteristic energy at which their spectra flatten is different by about a factor of $\geq 3$: $QPO_1$ reaches its peak at around $\sim 6$ keV, while $QPO_2$ is much harder and peaks at $\gtrsim 20$ keV.

3. The time lags of the two peaks are different: $QPO_1$ has soft lags (the soft X-rays lag behind the hard ones), while $QPO_2$ has hard lag (Casella et al. 2004). This property is a definition of type-B QPOs (e.g. Remillard et al. 2002; Casella et al. 2005).

4. The value of the bicoherence $b^2(\nu_2, \nu_1)$ is compatible with statistical noise, which tends to indicate a very weak or no coupling between the peaks at $\nu_2$, $\nu_1$, and $\nu_1 + \nu_2$.

While points 2, and 3 have been mentioned for other BHBs (e.g. Homan et al. 2001; Rao et al. 2010; Cui 1999, for XTE J1550−564 and GRS 1915+105), in addition to XTE J1859+226 (Casella et al. 2004), it is the first time to our knowledge that points 1 and 4 are reported for any BHBs. In XTE J1550−564 Heil et al. (2011) report a positive linear RMS-flux relation for (type-C) QPOs with a frequency smaller than $\sim 4$ Hz, and a negative RMS-flux trend at higher frequencies. Here the situation is opposite. $QPO_2$, that has the highest frequency, shows the linear relation, and $QPO_1$ shows the negative trend (Fig. 3). This could be the signature of a new fundamental difference between types B and C QPOs.

In XTE J1550−564, Rao et al. (2010) mentioned that the difference of energy spectra of the two peaks, especially the fact that the fundamental has a higher amplitude at high energy can indicate a more sinusoidal signal at higher energies. In this respect, the fact that $QPO_1$ is stronger at low flux could also indicate a more sinusoidal signal in the peaks. This explanation, although simple and tempting, do not account for the different signs of the time lags of the two peaks, since one would naively expect in the case of a non-purely sinusoidal signal that all components undergo the same physical processes and thus show similar lags.

In addition, Rao et al. (2010) come to the conclusion that the peak referred to as sub-harmonic in XTE J1550−564 could in fact be the true fundamental feature. In this case the "more sinusoidal" explanation does not hold any more since the harmonic (and therefore the peak with the highest frequency) should then disappear first, and show a softer spectra, which is clearly opposite to what is seen here.

It is interesting to remark, here, that the bicoherence behavior of the two peaks (at $(\nu_1, \nu_1)$ and $(\nu_2, \nu_2)$) is similar to that of the type C QPOs of GRS 1915+105 (Maccarone et al. 2011), where $b^2$ reaches a high value close to the frequencies of the peaks. In this latter source $b^2$ is high at the (bi-)position of the fundamental, and much lower for the harmonic (Maccarone et al. 2011). Pursuing the comparison with GRS 1915+105, in XTE J1859+226 the values of $b^2$ would tend to indicate that $QPO_1$ is the fundamental and $QPO_2$ its harmonic. In this latter source, however, different global patterns have been identified in the bichorence plot. In all cases (where a strong harmonic is seen) a strong coupling is seen between the fundamental and the harmonic (e.g. the "web" or "cross" patterns Maccarone et al. 2011), and even between the noise component and the QPO. This is not observe in the case of XTE J1859+226 (Fig. ref-fig:bicoh).

An easy interpretation for the four points above would be that the two peaks have absolutely no relation together and that the apparent harmonic relation of their frequencies is fortuitous. This seems difficult to reconcile with the fact that a similar behavior is seen both in Obs. 1 and 2 that are separated by roughly a day, and a transition into another state (Casella et al. 2004). In addition, point 2 in the case of type C QPOs, and points 2 and 3 in the case of type B QPOs have been reported in this and other sources (Cui 1999; Homan et al. 2001; Remillard et al. 2002; Rodriguez et al. 2002a; Casella et al. 2004; Rao et al. 2010). It is more likely that the two peaks are somehow related or that, at least, a possible common mechanism sets their frequencies to be integer multiple, with the two features not being harmonics in a physical sense.

Hard lags are usually easy to understand in the context of Comptonization of soft photons in a hot and tenuous medium (e.g. the so-called corona; e.g. Cui 1999). As discussed in Cui (1999), and Gierliński & Zdziarski (2005) the energy dependences of both the QPO and/or the continuum are indicative of variations of physical parameters: the favored ones are either the temperature and/or optical depth of the corona (Cui 1999), the temperature of the soft photons, or a variable power of the Comptonized component (Gierliński & Zdziarski 2005). In this respect, however, the different time dependences of the two peaks, and the opposite sign of their time lags are difficult to understand.

Other families of models involve precession at the inner boundary of the disk, but here again, the fundamental and harmonics are produced at the same location and should 'see' the same environment. In the framework of Comptonization the time lags, RMS-spectra, and bicoherence of the different features should be the same.

A way to possibly reconcile the four points summarized above could be that the peaks are not harmonics in the

usual sense but that they represent different modes of the same mechanism favored at different moments, depending of some (unknown) parameter(s) in the corona-disk-jet system. This hypothesis has the advantage of providing an explanation for the time behavior of the two peaks, and permits in particular that they do not necessarily appear at the same time, but enter in a sort of competition. The competition has also been mentioned for other types of QPOs in XTE J1859+226 by Casella et al. (2004) and in the case of XTE J1550−564 by Remillard et al. (2002) although it has never been explored further. The physical states of the disk/corona/jet system might then set the conditions for one or the other peak to dominate. This will be explored by us from a particular theoretical standpoint in a forthcoming paper (Varnière, Tagger, Rodriguez, submitted to A&A). we note that the behavior observed in the case of the cathedral QPO is different from, at least, that of the type C QPO of GRS 1915+105 with respect to the RMS-flux relation and to the bicoherence behavior (Heil et al. 2011; Maccarone et al. 2011). This may, however, represent a fundamental property of type B QPOs in general. In any cases, the new model-independent observational facts presented here should be taken as strong constraints in any attempts to model LFQPOs in BHBs.

REFERENCES

Berger, M. & van der Klis, M. 1994, A&A, 292, 175
Brocksopp, C., Fender, R. P., McCollough, M., et al. 2002, MNRAS, 331, 765
Casella, P., Belloni, T., Homan, J., & Stella, L. 2004, A&A, 426, 587
Casella, P., Belloni, T., & Stella, L. 2005, ApJ, 629, 403
Cui, W. 1999, ApJ, 524, L59
Cui, W., Shrader, C. R., Haswell, C. A., & Hynes, R. I. 2000, ApJ, 535, L123
Gierliński, M. & Zdziarski, A. A. 2005, MNRAS, 363, 1349
Heil, L. M., Vaughan, S., & Uttley, P. 2011, MNRAS, 411, L66
Homan, J. & Belloni, T. 2005, Ap&SS, 300, 107
Homan, J., Wijnands, R., van der Klis, M., et al. 2001, ApJS, 132, 377
Ingram, A., Done, C., & Fragile, P. C. 2009, MNRAS, 397, L101
Maccarone, T. J. & Coppi, P. S. 2002, MNRAS, 336, 817
Maccarone, T. J., Uttley, P., van der Klis, M., Wijnands, R. A. D., & Coppi, P. S. 2011, MNRAS, 251
Mikles, V. J., Varniere, P., Eikenberry, S. S., Rodriguez, J., & Rothstein, D. 2009, ApJ, 694, L132
Molteni, D., Sponholz, H., & Chakrabarti, S. K. 1996, ApJ, 457, 805
Muno, M. P., Morgan, E. H., & Remillard, R. A. 1999, ApJ, 527, 321

Rao, F., Belloni, T., Stella, L., Zhang, S. N., & Li, T. 2010, ApJ, 714, 1065
Remillard, R. A. & McClintock, J. E. 2006, ARA&A, 44, 49
Remillard, R. A., Sobczak, G. J., Muno, M. P., & McClintock, J. E. 2002, ApJ, 564, 962
Rodriguez, J., Corbel, S., Hannikainen, D. C., et al. 2004a, ApJ, 615, 416
Rodriguez, J., Corbel, S., Kalemci, E., Tomsick, J. A., & Tagger, M. 2004b, ApJ, 612, 1018
Rodriguez, J., Durouchoux, P., Mirabel, I. F., et al. 2002a, A&A, 386, 271
Rodriguez, J., Shaw, S. E., Hannikainen, D. C., et al. 2008, ApJ, 675, 1449
Rodriguez, J., Varnière, P., Tagger, M., & Durouchoux, P. 2002b, A&A, 387, 487
Shaposhnikov, N. & Titarchuk, L. 2007, ApJ, 663, 445
Tagger, M. & Pellat, R. 1999, A&A, 349, 1003
Uttley, P., McHardy, I. M., & Vaughan, S. 2005, MNRAS, 359, 345
Varnière, P., Tagger, M., & Rodriguez, J. 2011, A&A, 525, A87+
Vignarca, F., Migliari, S., Belloni, T., Psaltis, D., & van der Klis, M. 2003, A&A, 397, 729
Wagoner, R. V., Silbergleit, A. S., & Ortega-Rodríguez, M. 2001, ApJ, 559, L25
Wood, A., Smith, D. A., Marshall, F. E., & Swank, J. 1999, IAU Circ., 7274, 1

TABLE 1

QPO PARAMETERS OBTAINED FROM THE FITS TO THE 2–40 keV PDS. THE ERRORS ARE GIVEN AT THE 90% LEVEL.

| Obs. # | $\nu_1$ (Hz) | $Q_1$[‡] | $A_1$[†] (% RMS) | $\nu_2$ (Hz) | $Q_2$[‡] | $A_2$[†] (% RMS) | $\nu_3$ (Hz) | $Q_3$[‡] | $A_3$[†] (% RMS) |
|---|---|---|---|---|---|---|---|---|---|
| 1 | $2.94 \pm 0.02$ | 5.9 | $2.8 \pm 0.1$ | $5.828 \pm 0.025$ | 7.3 | $4.7 \pm 0.1$ | $11.2^{+0.3}_{-0.4}$ | 9.5 | $1.1^{+0.2}_{-0.3}$ |
| 2 | $3.00 \pm 0.04$ | 5.2 | $2.9 \pm 0.2$ | $5.86 \pm 0.04$ | 6.5 | $4.6^{+0.2}_{-0.1}$ | $11.5 \pm 0.3$ | 8.3 | $1.5^{+0.2}_{-0.3}$ |

[‡] $Q = \nu/\text{FWHM}$.

[†] $A$ stands for RMS amplitude.

Rodriguez & Varnière

Fig. 1.— Upper panel: 2–40 keV dynamical power spectrum of XTE J1859+226. Lower panel: 2–40 keV light curve.
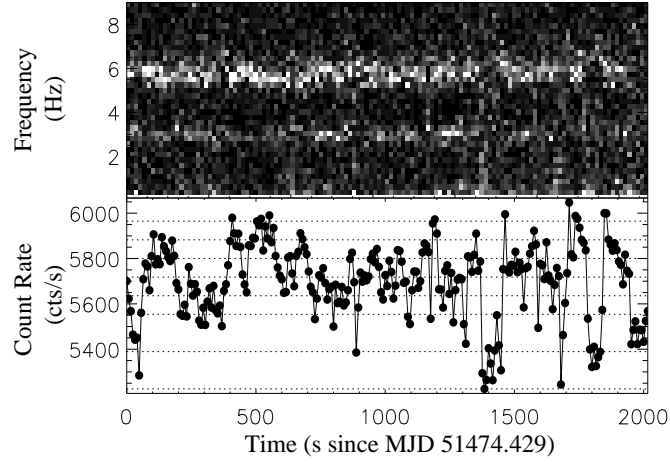


Fig. 2.— 2–40 keV power spectra showing the presence of the 'cathedral' QPO, the best fit model, and the single components used in the fit. The solid lines show the thin features (QPO and harmonic), the dashed line show the continuum component (including the white noise).
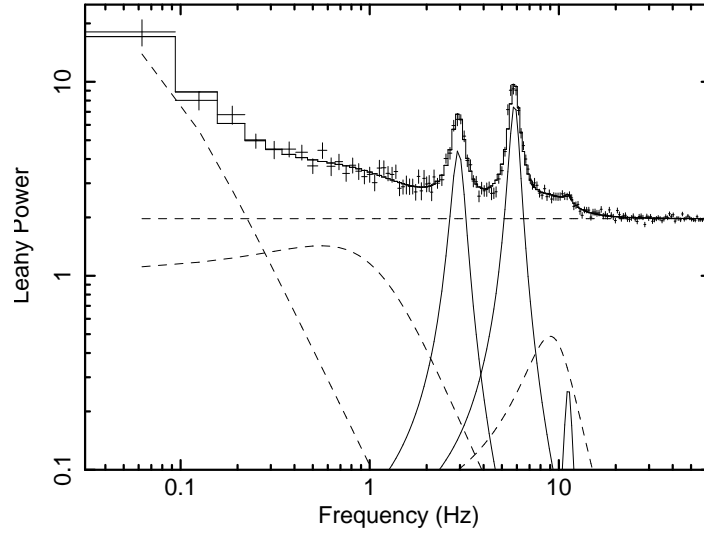


Fig. 3.— Evolution of the QPOs absolute amplitudes with the count rate for Obs. 1. The diamonds correspond to $QPO_1$ and the circles to $QPO_2$.
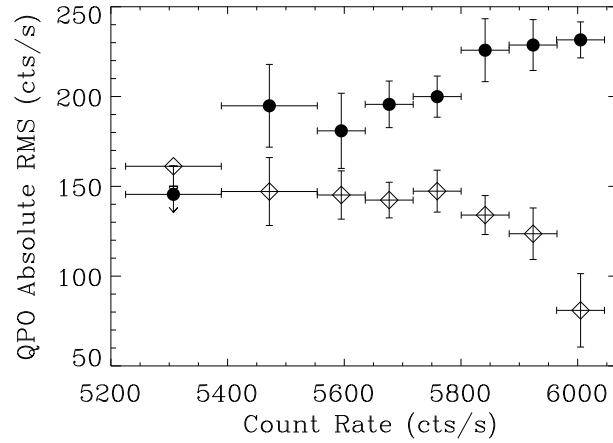
FIG. 4.— **Left:** Energy dependences of the two main QPOs. Upper limits are given at the 90% level. **Right:** Ratio between the amplitudes of $QPO_2$ and $QPO_1$.
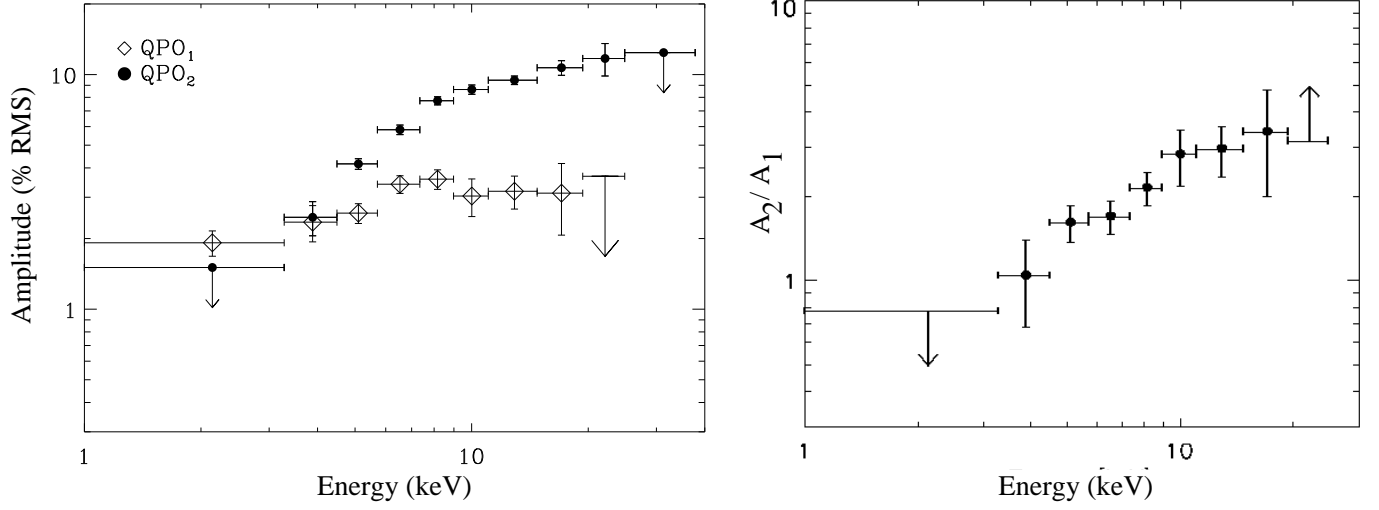


FIG. 5.— Bicoherence plot for Obs. 1 on a frequency region including the two peaks. The white regions are $5 \times 5$ pixels boxes centered on the positions of the two peaks (at respectively $\sim (2.94, 2.94)$ Hz and $\sim (5.83, 5.83)$ Hz), while the black one is centered on $\sim (5.83, 2.94)$ Hz and shows the value of $b^2$ at the intersection of the two peaks.